REPORT DOCUMENTATION PAGE

Form Approved

OMB No. 0704-0188

1. REPORT DATE *(DD-MM-YYYY)*	2. REPORT TYPE	3. DATES COVERED *(From - To)*
14-07-2015	Final	01-June-2014 to 31-May-2015

4. TITLE AND SUBTITLE

Investigation of Chirality Selection Mechanism of Single-Walled Carbon Nanotube

5a. CONTRACT NUMBER
FA2386-14-1-4047

5b. GRANT NUMBER
Grant 14IOA058_144047

5c. PROGRAM ELEMENT NUMBER
61102F

6. AUTHOR(S)

Dr. Seung Min Kim

5d. PROJECT NUMBER

5e. TASK NUMBER

5f. WORK UNIT NUMBER

7. PERFORMING ORGANIZATION NAME(S) AND ADDRESS(ES)

Korean Institute of Science and Technology
Eunhari San 101, Bongdong-eup, Wanju-gun
Jeonbuk 565-905
Korea

8. PERFORMING ORGANIZATION REPORT NUMBER

N/A

9. SPONSORING/MONITORING AGENCY NAME(S) AND ADDRESS(ES)

AOARD
UNIT 45002
APO AP 96338-5002

10. SPONSOR/MONITOR'S ACRONYM(S)

AFRL/AFOSR/IOA(AOARD)

11. SPONSOR/MONITOR'S REPORT NUMBER(S)

14IOA058_144047

12. DISTRIBUTION/AVAILABILITY STATEMENT

Distribution Code A: Approved for public release, distribution is unlimited.

13. SUPPLEMENTARY NOTES

14. ABSTRACT

This project involved investigation of two significant mechanistic aspects of carbon nanotube (CNT) array growth under chemical vapor deposition conditions: chirality selectivity and termination. The research involved development of a “proper” Transmission Electron Microscopy (TEM) sample preparation method that allowed direct observation of interfaces between CNTs and catalyst layers and lead to optimized growth conditions for synthesis of short, less dense, and highly crystalline single-walled carbon nanotubes. Based on ex-situ and in-situ TEM investigation, a modified growth termination model was proposed to better explain various phenomena of carbon nanotube growth and growth termination. The results strongly suggest that growth termination of CNT forests is affected by the morphological evolution of catalyst particles.

15. SUBJECT TERMS

Carbon Nanotubes, Chirality, Processing, Catalysis, Mechanism, Growth, Termination

16. SECURITY CLASSIFICATION OF:			17. LIMITATION OF ABSTRACT	18. NUMBER OF PAGES	19a. NAME OF RESPONSIBLE PERSON
a. REPORT	b. ABSTRACT	c. THIS PAGE			Kenneth Caster, Ph.D.
U	U	U	SAR	19	19b. TELEPHONE NUMBER *(Include area code)* +81-42-511-2000

Standard Form 298 (Rev. 8/98)
Prescribed by ANSI Std. Z39.18

Final Report for AOARD Grant FA2386-14-1-4047

"Investigation of chirality selection mechanism of single-walled carbon nanotube"

Date: 7/17/2015

PI and Co-PI information:

- Name of Principal Investigator: Seung Min Kim
- E-mail address: seungmin.kim@kist.re.kr
- Institution: Korea Institute of Science and Technology
- Department: Carbon Composite Materials Research Center
- Mailing Address: Chudong-ro 92, Bongdong-eup, Wanju-gun, Jeonbuk 565-905, South Korea
- Phone: +82-63-219-8154
- Fax: +82-63-219-8419

Period of Performance: 6/1/2014 ~ 5/31/2015

Abstract:

In the first year of the project, we have taken an effort to investigate two significant aspects of carbon nanotube synthesis: chirality selection of single-walled carbon nanotube and growth termination of carbon nanotube array. In order to successfully study two issues, we have first focused on the development of a "proper" TEM sample preparation method and demonstrated that a focused ion beam based method worked very well for our research purpose. Therefore, based on the developed TEM sample preparation method, we tried to investigate a chirality selection mechanism of single-walled carbon nanotube, but we have found out that not only the proper TEM sample preparation but also, more importantly, the optimization of growth conditions for synthesis of short, less dense, and highly crystalline single-walled carbon nanotubes is highly required. This work will continue in the second year of the project. In addition, the investigation on the growth termination of CNT array using the developed TEM sample preparation method has been performed and the result was very interesting. Based on ex-situ and in-situ TEM investigation, we proposed a modified growth termination model to better explain various phenomena of carbon nanotube growth and growth termination. In the second year of the project, we will confirm our growth termination model and perform rational designs of catalyst layers for extremely long catalyst lifetime.

Introduction:

Carbon nanotubes (CNTs) exhibit exceptional physical and mechanical properties, which have been drawing significant attention from academic societies as well as industries. For examples, CNTs are 100 times stronger than steel at only one sixth of the weight, and conduct electric current three orders magnitude higher than conventional metals [1-3]. For SWCNTs, the electronic properties can vary between semiconducting and metallic depending on their structures (as known as their chirality). Based on the exceptional properties of CNTs, various potential applications such as field emitters [4], biosensors [5], strong fibers [6, 7], membranes [8], and super-capacitor electrodes [9] have been proposed and demonstrated in a laboratory environment. However, the realization and commercialization of these CNT-based applications in the industry have not been successful so far, mainly due to lack of control over their structures (e.g. length, diameter, crystallinity, number of walls, etc), yield and chirality during large-scale synthesis. Especially, the control of SWCNT's chirality selection and continuous synthesis of CNT arrays with infinite length have been two ultimate goals in CNT synthesis research since its discovery. In order to accomplish two ultimate goals, it is highly required, in advance, to thoroughly understand the chirality selection mechanism of SWCNTs and the growth termination mechanism of CNT arrays.

For chirality selection mechanisms of SWCNTs, the experimental approaches as well as theoretical calculations have been performed. The selective growth of nearly 90 and 96% of semiconducting tubes, respectively, by plasma enhanced chemical vapor deposition (PECVD) has been reported [10, 11]. However, an exact mechanism how plasma in reaction gas ambient leads to semiconducting tube dominance is still unclear. A. R. Harutyunyan, et al. [12] showed that by adjusting catalyst pre-treatment conditions the ratio of metallic to semiconducting tubes can be altered from 18% to 91%. In addition, they observed in-situ the evolution of catalyst shapes and size distributions depending on pre-treatment conditions using environmental-cell transmission electron microscope (E-TEM) and correlated catalyst morphology changes with metallic tube selectivity. W. -H. Chiang and R. H. Sankaran [13] developed a catalyst synthesis method, which produces uniformly sized catalyst particles with various compositions of Ni and Fe, so they can exclude the effect of catalyst particle sizes and only investigate the effect of catalyst particle compositions. They showed that the distribution of SWCNT chiralities evolved with compositions of catalyst particles. These two works made significant advances in understanding chirality selection mechanism. However, in these two works, they investigated

SWCNTs with Raman, photoluminescence, or absorption spectroscopy but catalyst particles with TEM, so structural correlations between SWCNTs and catalyst particles have been established in indirect way. Structural determination of SWCNT chirality by high resolution imaging [14] and diffraction [15] using TEM has been demonstrated but simultaneous investigation of both SWCNTs and catalyst particles has not been reported. Theoretical calculation predicted that SWCNTs with some specific chiralities are energetically favorable for Ni(111) surface [16] based on epitaxial relationship, but no experimental evidence has directly supported this calculation so far. Previous results strongly suggest that there may be strong correlations between catalyst structures and SWCNT chiralities, but no experimental result so far has shown the direct correlation between them.

For growth termination mechanisms of CNT arrays, there have been far more advances in the understanding of CNT growth termination phenomena compared to chirality selection mechanism, because it is more practical issue. In the last decade, several growth termination mechanisms of CNT forests have been proposed in order to explain certain features of growth and growth termination, such as abrupt growth termination [17], growth enhancement by water vapor [18-20], and the temperature dependence of growth termination [21, 22]. Recently, a study concerning long-length CNT forests [23] confirmed that there is the inverse dependence of growth termination or catalyst lifetime on the growth temperature and flow rates of carbon precursor, the two most important parameters in CNT forest growth. Catalyst lifetime is known to depend on the relative amount of carbon in the carbon precursor, and this can be explained by the growth termination mechanisms of amorphous carbon poisoning [18, 19] in which the growth of CNT forest is terminated by deactivated catalysts covered by amorphous carbon, or by carbide formation [24]. However, these mechanisms cannot explain the growth temperature dependence. On the other hand, Ostwald ripening and sub-surface diffusion induced growth termination [20-22, 25] do explain the growth temperature dependence, because both Ostwald ripening and sub-surface diffusion are thermally activated processes. However, it is difficult for this growth termination mechanism to account for the observed effect of differing carbon contents in the precursor. Thus, to date, there has been no single growth termination mechanism that can explain all of the features of CNT forest growth.

For both chirality selection mechanism and growth termination mechanism studies, the most effective way is to directly observe the interface between CNTs and catalyst particles. Thus, in the first year of the project, we have first focused on the development of transmission electron

microscopy (TEM) sample preparation method, which enables us to directly observe the interfaces between carbon nanotubes (CNTs) and metal catalyst particles. We have proposed two methods: catalysts on ceramic beads and focused ion beam (FIB) based method. We found out that FIB based method works much better than the method using catalysts on ceramic beads for our research purpose. Then, we have taken the efforts on attaining high-resolution TEM images of the interfaces between CNTs and metallic catalysts in order to investigate the structural correlation between CNTs and metallic catalysts. However, we realized that there are a few problematic issues in the approach, which we performed in the first year of the project. Nevertheless, throughout the developed FIB based TEM sample preparation method and in-situ and ex-situ TEM investigation, we have obtained important knowledge related to the growth termination mechanism of CNT arrays.

Experiment:

- Growth of CNT forests on Si wafer and TEM investigation

A silicon wafer (P/Boron (100) type) was used as a substrate. The substrate was coated with 10-30 nm of Al_2O_3 film at the rate of 0.02 nm/s and 0.5 nm of Fe film at the rate of 0.01 nm/s using e-beam evaporation. A piece of the catalyst-coated substrate was inserted in the middle of a quartz tube whose inner diameter was 46 mm. The temperature was ramped to 740 °C in 15 minutes at low pressure (base pressure: 5×10^{-7} Torr). When the temperature reached 740 °C, a gas mixture of C_2H_2 (2 sccm), H_2 (400 sccm), water vapor (5 mTorr) was fed for 4 and 30 minutes to grow the CNT forest. Hot filament was turned on only for the initial 4 minutes. During the growth process, the pressure was measured to be 2 Torr.

Standard TEM sample preparation methods have been utilized. For cross-sectional samples, the sample was stacked together with dummy silicon pieces using Gatan G-1 Epoxy and then hand-polished on one side. After finishing one side, the other side was also back-polished and then dimpled down to 5-10 μm at the center. Then, the sample was ion-milled from both sides at 4.5° angle and at 4.5 kV using Gatan PIPS™ until the small hole at the center of the sample was made.

- Growth of CNT forests on thin membrane

The 3 mm by 3 mm pieces of Si wafer with 500 nm thick thermally grown SiO_2 were stacked together using Gatan G-1 Epoxy and then hand-polished on one side. After finishing one side,

the other side was also hand-polished until the sample thickness was thinned down to 40 μm. The half-ring grid was bonded to the samples for safe handling. The samples were loaded in a focused ion beam (FIB) and milled until 100 nm thick windows were made. Then, the samples were loaded in e-beam evaporator and 30 nm Al_2O_3 and 0.5 nm Fe layers were deposited on the edge of the membrane by e-beam evaporation at the rate of 0.02 nm/s and 0.01 nm/s, respectively. The CNT growth was performed in the same way as the CNT growth on the catalyst-coated Si wafer using the water-assisted HF-CVD. For ex-situ TEM investigation, the membrane was directly loaded and investigated in the TEM without additional sample preparation.

For in-situ investigation, E-TEM experiments were performed by 're-growing' the CNTs from a membrane sample. Initially, CNT forest was grown on a membrane sample for 3.5 minutes ex situ, and the sample was subjected to a similar growth condition in the E-TEM. We ramped up the temperature up to 700 °C in 5 minutes under 0.4 Torr of H_2 and waited for an additional 10 minutes for stabilization of the sample. Then, we added 2×10^{-3} Torr of C_2H_2 to the 0.4 Torr of H_2 just before we recorded the video.

Results and Discussion:

- Development of "new" TEM sample preparation method

Development of a sample preparation method for observing the interfaces between CNTs and catalyst particles without any damage induced by the conventional post-TEM sample preparation method has been first performed. We have tested two methods: catalysts deposited on ceramic beads FIB based method. As shown in Figure 1a, Pd catalysts on Al_2O_3 beads lead to the growth of carbon structures, but these are not single-walled CNTs (SWCNTs), which have definite chiralities. We have tried to optimize growth conditions for SWCNTs, but it was not quite successful. We believe that the failure to produce SWCNTs from catalysts on ceramic beads is not caused by catalyst-support structures. This is more likely to be caused by improper catalysts for SWCNT growth. Only Pd and Pt catalysts on Al_2O_3 were available for the growth. Thus, if we can get Fe/Al_2O_3 beads, this method would work much better. On the contrary to catalysts on bead method, FIB based method produced well-aligned array of CNTs as shown in Figure 1b. Therefore, all of the experiments in the first year of the project were performed using FIB based method.

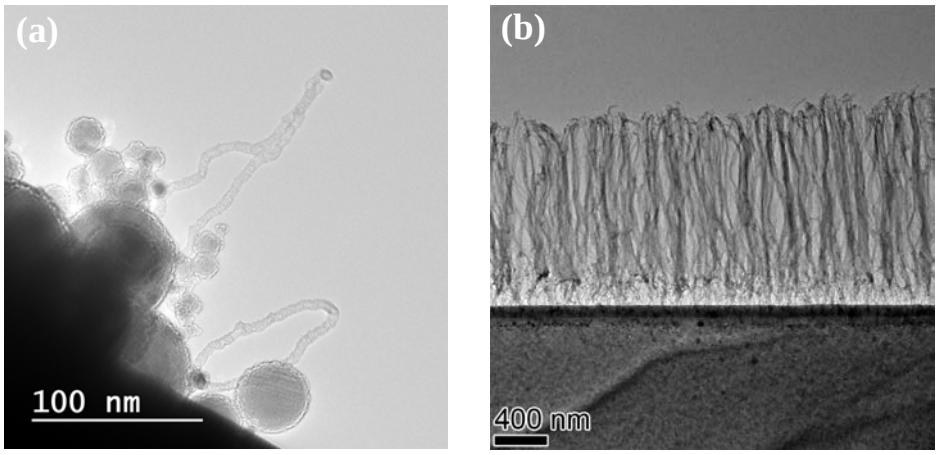

Figure 1. Growth of CNTs on (a) Pd/Al_2O_3 bead catalysts and (b) Fe/Al_2O_3 deposited thin membrane prepared by FIB based method

- Investigation of chirality selection mechanism of single-walled carbon nanotube

Based on FIB based method, CNTs were grown on Fe/Al_2O_3 deposited membranes for several different time periods. The growth condition where the growth of the SWCNTs and double-walled CNTs (DWCNTs) was confirmed with Fe/Al_2O_3/Si samples using a hot-filament assisted chemical vapor deposition (CVD). A representative TEM image of the interface between CNTs and catalysts is shown in Figure 2a. The image in Figure 2a clearly shows that SWCNTs are synthesized and the interfaces are clearly visible. However, high-resolution image of the interface between the CNT and the catalyst particle for the investigation of the structural correlation between CNTs and catalyst particles was hardly acquired. There are a few reasons. As shown in Figure 2a, some of the CNTs (arrowed) do not have catalyst particles at the base. Figure 2b indicates that some of catalyst particles are lifted up in the array of CNTs. Also, some of catalyst particles should be dissolved out by Ostwald ripening and subsurface diffusion as reported earlier by our group[]. Thus, in this case, it is obvious that we cannot get high-resolution images. In many other cases, the density of CNTs is too high to get high-resolution TEM image of individual CNT and catalyst particle. It is very hard to properly focus due to overlapped CNTs and catalyst particles. Therefore, we realized that it is highly required to first optimize the growth condition where less dense and very short SWCNTs can be produced. This is the critical factor for successfully investigating the structural correlation between CNTs and catalyst particles.

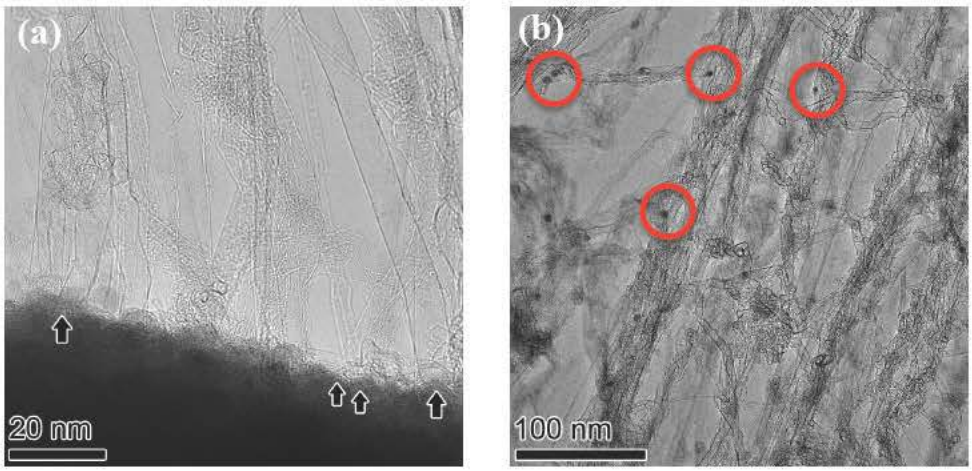

Figure 2. TEM images of (a) the interface between CNTs and catalyst particles and (b) CNT array of the Fe/Al_2O_3 membrane sample after CNT growth for 10 minutes.

- Growth termination mechanism of CNT arrays

In order to investigate growth termination mechanisms of CNT arrays, CNT forests were grown on the membrane samples for various growth times. As shown in Figures 3a and 3b, the growth was not fully initiated in 3 minutes, but by 3.5 minutes, the CNTs nucleated and the forest structure started to form. This means that at least 3 minutes is required for the nucleation step in our CNT forest growth. The relatively long nucleation time is attributed to our growth procedure in which the pre-heated furnace is translated to the sample such that the sample is located in the middle of the furnace in order to minimize the aggregation of catalyst particles. Thus, a certain time would be required for heat transfer and subsequent catalyst particle formation, but it is otherwise faster than the normal heating rate of a tube furnace. As presented in Figures 3c and d, the height of the SWCNT forest increases with growth time up to 10 minutes, indicating that CNT forest growth is successfully reproduced with the membrane samples. For growth times longer than 10 minutes, the length of CNT forest is too long for TEM observation, and thus we limit the growth time to 10 minutes.

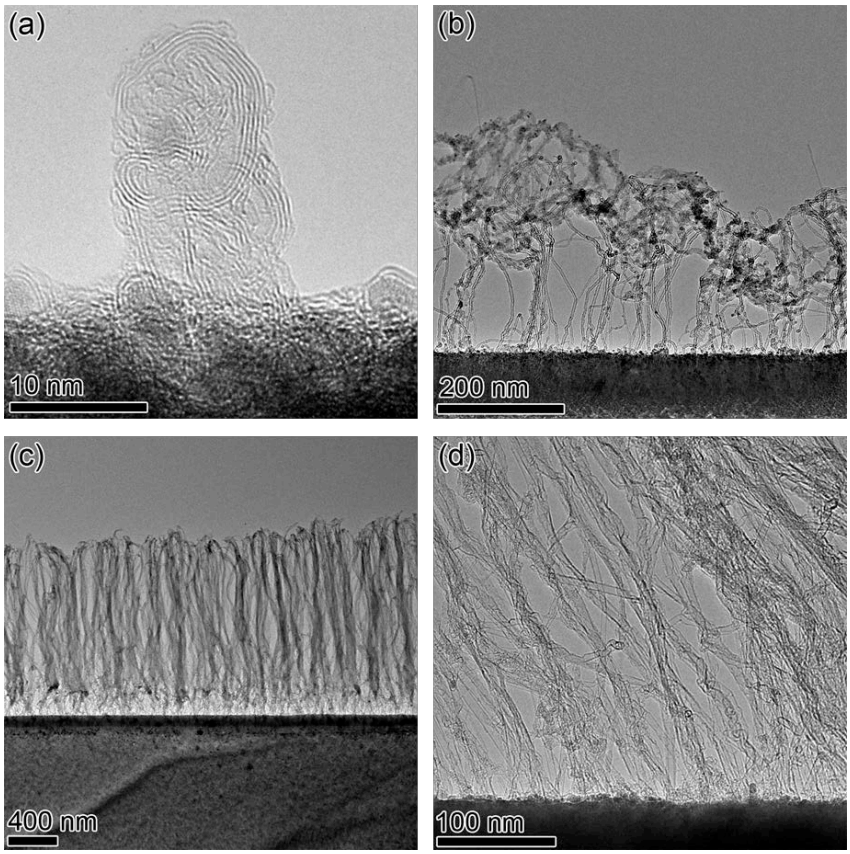

Figure 3. TEM images of the membrane samples after growing CNT forests for (a) 3 min, (b) 3.5 min, (c) 5 min, and (d) 10 min at 740 °C. (Note: each image has a different scale bar)

Figures 4a and b show high resolution TEM images of the interfaces between CNT forests and catalyst and support layers for the membrane samples after growting CNT forests for 3.5 and 10 minutes. The clear difference between the samples after 3.5 minutes of growth and 10 minutes of growth in Figures 4a and b is the number density of catalyst particles. The 3.5 minute growth sample in Figure 4a has a higher number density of catalyst particles in comparison with the 10 minute growth sample shown in Figure 4b. Some of catalyst particles in Figure 4a have been lifted up from the support layer along with the growing carbon structures. In Figures 4b and c, several CNTs (indicated by the arrows) do not have catalyst particles at their base, meaning that these CNTs no longer grow as a result of the loss of their catalyst particles. In previous studies, our group has claimed that the loss of catalyst particles is induced by Ostwald ripening and sub-surface diffusion [20-22, 25], which eventually leads to the termination of CNT forest growth. In Figures 4d and e, several interesting features are observed in the CNT arrays. Some catalyst particles (indicated by red circles in Figures 4d and e) reside within the CNT arrays,

even though it is well known that CNTs grow from Fe/Al_2O_3/Si substrates in the base growth mode [26]. Figure 4f shows a high resolution TEM image of a catalyst particle residing in the CNT arrays in the Figure 4d, clearly revealing the crystal structrue of the catalyst particle. However, the fact that catalysts are observed to be embedded within the CNT array does not necessarily mean that CNTs in this system grow in the tip growth mode: many more catalyst particles are seen at the base of the forest, and those catalysts that have lifted up from the substrate are not present at the tips of the CNTs. It seems most probable for catalyst particles to climb up in the CNTs during the growth, even though CNTs start to grow in the base growth mode.

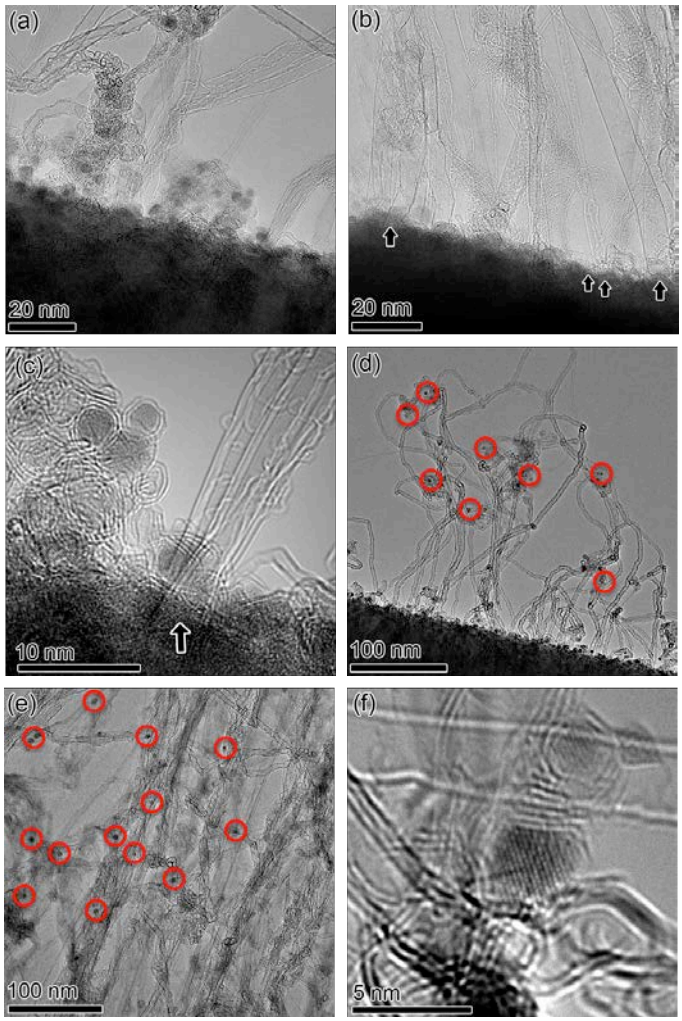

Figure 4. High resolution TEM images of the interfaces between CNT forests and catalyst and support layers for the samples grown for (a) 3.5 and (b) 10 minutes. (c) Magnified TEM image of CNTs without catalyst particles at the base in (a). TEM images showing the lifted catalysts in

the CNT arrays for the samples grown for (d) 3.5 and (e) 10 minutes. (f) Magnified TEM image of the lifted catalyst particles in (d).

In order to determine the mechanism by which catalyst particles exist in bulk of the CNT forest, we performed real time growth experiment in situ in an environmental transmission electron microscope (E-TEM). In order to mimic the geometry of the CNT forest described above, we performed the E-TEM experiments by 're-growing' the CNTs from a membrane sample where an initial CNT forest was grown for 3.5 minutes ex situ, and then subjected to a similar growth condition in the E-TEM. We ramped up the temperature up to 700 °C in 5 minutes under 0.4 Torr of H_2 and waited for an additional 10 minutes for stabilization of the sample. Then, we added 2×10^{-3} Torr of C_2H_2 to the 0.4 Torr of H_2 just before we recorded the video. Figure 6 shows six frames captured from the movie. In Figures 5a and b, the particle "1" starts to climb up from the substrate through the CNT walls. In addition, in Figures 5c, and d, other catalyst particles "2", and "3" climb up. In Figures 5e and f, two more catalyst particles "4" and "5" move from the left side of the TEM image and eventually catalyst particles "1", "2", "4" and "5" meet each other, and coalesce together to form a larger particle (Figure 5f). Compared to catalyst particles on the Al_2O_3 support layer, the catalyst particles that climb up into the CNT forests move easily, with a broadly random motion. This is most likely because the interaction between the CNT walls and the catalyst particles is weak. Thus, center-of-mass movement of particles is the mechanism by which the particles climb up through CNTs.

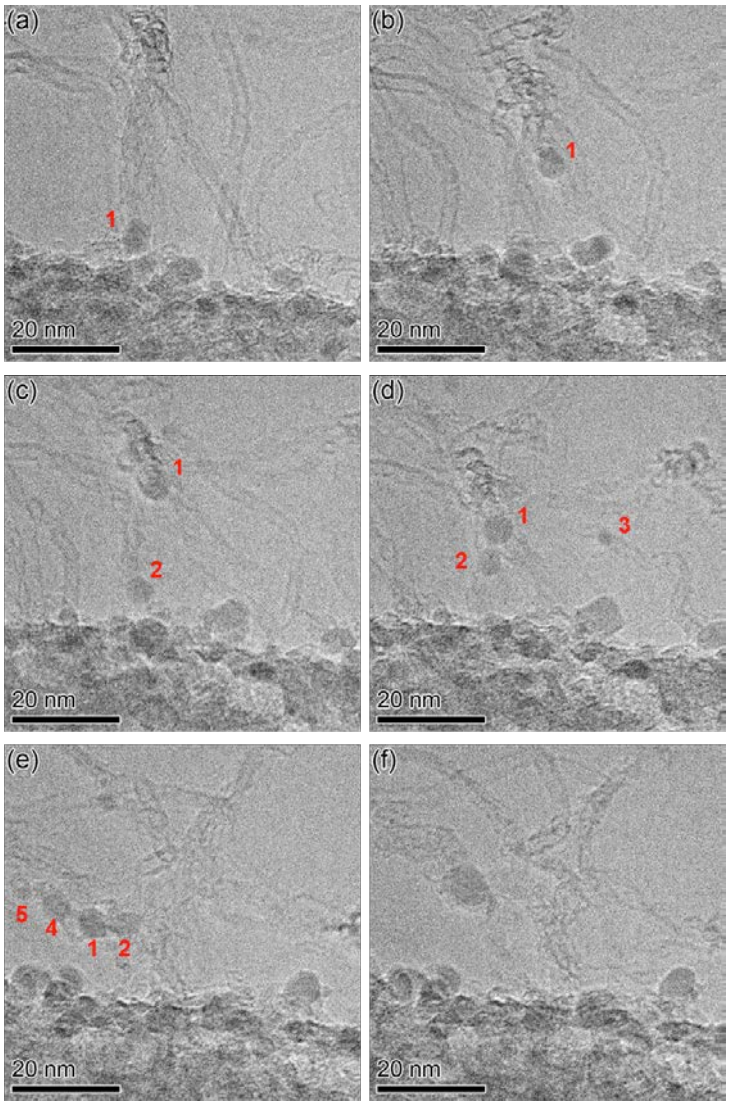

Figure 5. Six subsequent snapshots (a)-(f) captured from the video recorded during in-situ TEM growth experiment showing that the catalysts climb up through CNT arrays and coalesce into a big particle. Time lapses after the frame (a) are (b) 14.78, (c) 18.76, (d) 22.55, (e) 35.33, and (f) 38.8 seconds.

Figure 6 is a series of frames from another movie and clearly shows how easily catalyst particles move through CNTs and even jump to neighboring CNTs. The catalyst particle “1” in Figure 6a sits on the outward wall of the CNT and is covered by a graphitic shell. In Figures 6b-e, particle “1” comes out of the graphitic shell, penetrates inside the CNT and subsequently moves upward into the array. Simultaneously, two other particles “2” and “3” in Figures 6a-d move downward through CNTs, so the direction of movement of catalyst particles is indeed random. In Figures 6f-h, particle “1” jumps to the neighboring CNT, returns to the CNT where it was

initially, and then resumes its motion up from the substrate. Therefore, the catalyst particles that have been lifted off of the substrate and into the CNT forest can not only move upwards or downwards, but also jump to adjacent CNTs.

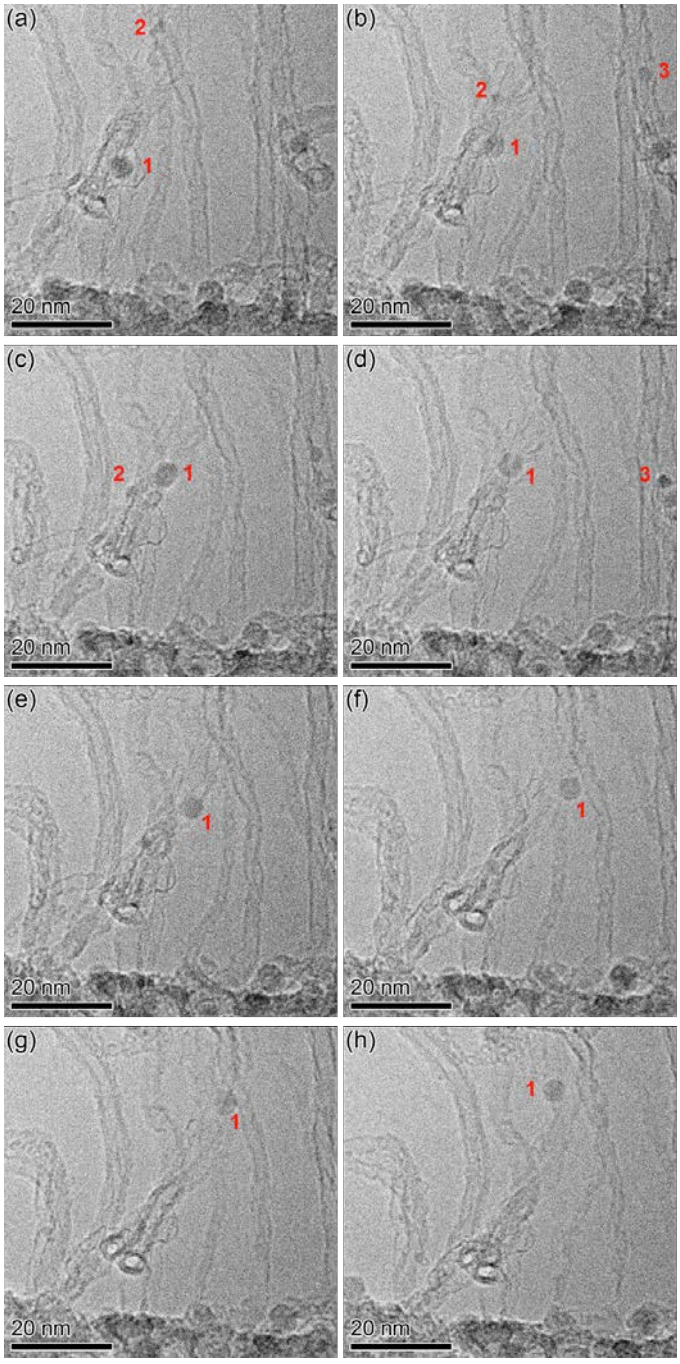

Figure 6. Eight subsequent snapshots (a)-(h) captured from the video recorded during in-situ TEM growth experiment showing the movement of the lifted catalysts. Time lapses after the frame (a) are (b) 5.07, (c) 7.65, (d) 8.5, (e) 9.75, (f) 13.0, (g) 15.5, and (h) 20.08 seconds.

In terms of uniform and stable growth of CNT forest, this observed migration of catalyst particles into the CNT forest is not a desirable phenomenon. We have observed through ex-situ and in-situ TEM investigations that some of those catalysts that have been lifted up into the forest subsequently nucleate and grow CNTs of their own. However, considering that most of studies regarding the efficient growth of CNT forest require a deposited Al_2O_3 layer as a support material [26-28] and the number of CNTs growing from the lifted catalysts are so low, the lifted catalysts from the support into CNT array should not contribute significantly to the overall forest growth compared to the remaining catalysts on Al_2O_3 support. Thus, as the number of lifted catalyst increases, the number density of growing CNTs decreases: this means that the lifted catalysts critically affect the process of growth and growth termination of the CNT forest, and contribute along with Ostwald ripening and sub-surface diffusion [20-22, 25] to the termination process. Thus, it remains a question as to why the catalyst particles migrate through CNT array and how significantly this process contributes to the overall termination process.

The nucleation and growth of CNTs on the metallic catalysts is driven by the chemical potential of supersaturated carbon inside the catalyst particle [29]. In the base growth mode, it is generally accepted that catalysts remain attached to the substrate during growth as a result of the strong surface interaction energy [29]. Because of this energetic preference, the direction of the carbon precipitation is towards the free surface rather than the interface between the catalyst and support layers. However, when the chemical potential energy of supersaturated carbon in the catalyst particle becomes high enough for some reasons, the precipitation of a new graphitic layer in between catalyst and support layers may be possible as observed in Figure 7a (indicated by an arrow). As soon as the catalyst particles are detached from the substrate due to the nucleation of a new graphitic layer at the catalyst/substrate interface, they are able to climb up the CNTs and move freely, as observed in Figures 5 and 6.

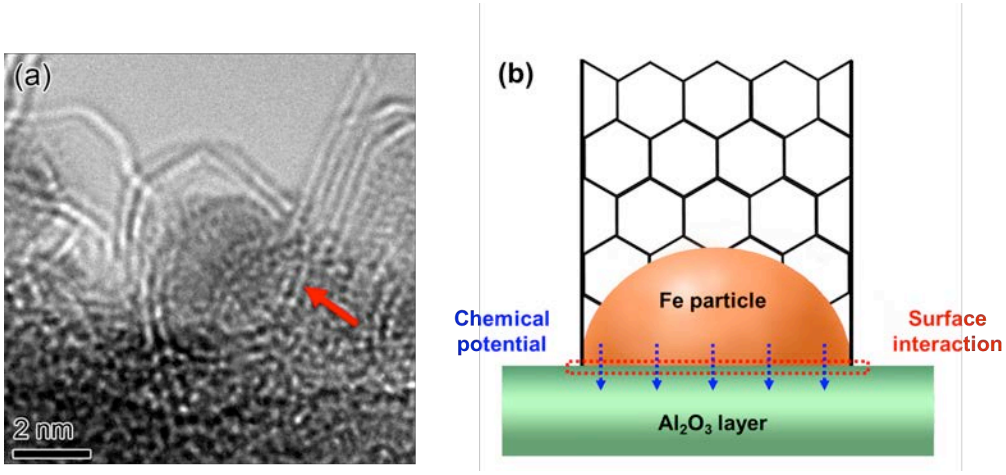

Figure 7. (a) High resolution TEM image of the catalyst particle, which nucleates and just starts to grow the CNT. The graphitic layers seem to cover the whole catalyst particle. (b) The schematic representation of an Fe particle on Al_2O_3 layer and two competing forces exerted on the Fe particle.

Based on the model shown in Figure 7b, we can construct a simple force balance equation between the chemical potential energy of supersaturated carbon and the surface interaction energy. The chemical potential energy of supersaturated carbon inside the Fe particle and surface interaction energy between the Fe particle and Al_2O_3 layer can be described as the following equations:

$$\textit{Chemical potential energy} = N_{C^*} k_B T \ln \frac{N_{C^*}}{N_{Fe} + N_{C^*}} - N_{C(0)} k_B T \ln \frac{N_{C(0)}}{N_{Fe} + N_{C(0)}}$$

$$\text{Surface interaction energy} = (\gamma_{iron} + \gamma_{alumina} - \gamma_{iron-alumina}) \times A$$

where N_{C^*} is the number of supersaturated C atoms, N_{Fe} is the number of Fe atoms, $N_{C(0)}$ is the number C atoms in Fe particles at the solubility limit, k_B is the Boltzmann constant, T is the temperature, γ_{iron} is the surface energy of Fe, $\gamma_{alumina}$ is the surface energy of Al_2O_3, $\gamma_{iron-alumina}$ is the interfacial energy between Fe and Al_2O_3, and A is the surface area between the iron particle and alumina.

In order to grasp the essential physics of this model, it is useful to consider the case where the energies of the Fe and Al_2O_3 surfaces and the Fe-Al_2O_3 interface are constant. Under this assumption, there are two factors that affect this balance equation: the number of supersaturated

carbon atoms (N_{C*}) and the size of catalyst particles (N_{Fe} and A). The number of supersaturated carbon atoms (N_{C*}) is generally well correlated with the flow of carbon precursor. Therefore, as either the carbon precursor flow increases or as the size of catalyst particles decreases, there would be much more chances for catalysts to be lifted up, resulting in shorter catalyst lifetime. This correlates with the observation that the catalyst lifetime reduces as the flow of carbon precursor increases [23]. Also, CNTs produced by long CNT forest growth with extremely long catalyst lifetime [23, 28] are usually multi-walled CNTs and deposited catalyst layers for long CNT growth are relatively thick, again consistent with this model.

Our experimental results strongly suggest that the growth termination of CNT forests is affected by the morphological evolution of catalyst particles. The observed lift-off of catalysts during growth works along with Ostwald ripening and sub-surface diffusion [20-22, 25] to strongly change the number density of catalyst particles available for CNT growth, thus leading to growth termination. In the early stages of CNT forest growth, Ostwald ripening dominates in reducing the catalyst density [22], but also smaller catalyst particles are also lifted up with the nucleation of CNTs. In this stage, most of very small particles either dissolve out or are lifted up. Then, in the later stage of growth, sub-surface diffusion dominates [22], but the number density of catalyst particles is well maintained for a longer period time. In this stage, CNT growth is very stable and the growth rate is almost constant. However, as the sizes of the catalyst particles continue to decrease due to sub-surface diffusion and at some point, the sizes of the catalysts cross the energy balance threshold and have an increased chance to be lifted up in the CNT arrays. The inclusion of this additional process in the overall understanding of growth termination not only better explains the observed dependence on growth temperature, but also the effect of carbon precursor flow rates on catalyst lifetime.

In conclusion, a complete picture of the evolution of the catalyst morphology during the CNT forest growth is provided by a combination of ex-situ and in-situ TEM investigation. We have developed a new TEM sample preparation methodology that allows direct observation of the interfaces between CNTs and catalyst layers. Based on these observations, we propose a modified growth termination model, in which the loss of catalysts from the substrate due to a ‘lift-up’ processes works synergistically with Ostwald ripening and sub-surface diffusion significantly to reduce the number density of catalyst particles available for CNT growth, leading to eventual growth termination. This modified model better explains the totality of observed phenomena related to the growth and growth termination of CNT forests.

Reference

[1] M. F. Yu, O. Lourie, M. J. Moloni, T. F. Kelly, and R. S. Ruoff, "Strength and breaking mechanism of multiwalled carbon nanotubes under tensile load," *Science*, **287**, 637 (2000).

[2] B. Q. Wei, R. Vajtai, and P. M. Ajayan, "Reliability and current carrying capacity of carbon naotubes," *Appl. Phys. Lett.*, **79**, 1172 (2001).

[3] P. L. McEuen, M. S. Fuhrer, and H. K. Park, "Single-walled carbon nanotube electronics," *IEEE Trans. Nanotechnol.*, **1**, 78 (2002).

[4] W. A. Heer, A. Châtelain, and D. A. Ugarte, "Carbon nanotube field-emission electron source," *Science*, **270**, 1179 (1995).

[5] C. Han, A. Doepke, W. Cho, V. Likodimos, A. A. de la Cruz, T. Back, W. R. Heineman, H. B. Halsall, V. N. Shanov, M. J. Schulz, P. Falaras, and D. D. Dionysiou, "A Multiwalled-carbon-nanotube-based biosensor for monitoring microcystin-LR in sources of drinking water supplies," *Adv. Funct. Mater.*, **23**, 1807 (2013).

[6] M. Zhang, K. R. Atkinson, and R. H. Baughman, "Multifunctional carbon nanotube yarns by downsizing an ancient technology," *Science*, **306**, 1358 (2004).

[7] K. Jiang, J. Wang, Q. Li, L. Liu, C. Liu, and S. Fan, "Superaligned carbon nanotube arrays, films, and yarns: a road to applications," *Advanced Materials*, **23**, 1154 (2011).

[8] B. J. Hinds, N. Chopra, T. Rantell, R. Andrews, V. Gavalas, and L. G. Bachas, "Aligned multiwalled carbon nanotube membranes," *Science*, **303**, 62 (2004).

[9] D. N. Futaba, K. Hata, T. Yamada, T. Hiraoka, Y. Hayamizu, Y. Kakudate, O. Tanaike, H. Hatori, M. Yumura, and S. Iijima, "Shape-engineerable and highly densely packed single-walled carbon nanotubes and their application as super-capacitor electrodes," *Nature Mater*. **5**, 987 (2006).

[10] Y. Li, D. Mann, M. Rolandi, W. Kim, A. Ural, S. Hung, A. Javey, J. Cao, D. Dunwei, E. Yenilmez, Q. Wang, J. F. Gibbons, Y. Nishi, and H. Dai, "Preferential growth of semiconducting single-walled carbon nanotubes by a plasma enhanced CVD method," *Nano Lett.*, **4**, 317 (2004).

[11] L. Qu, F. Du, and L. Dai, "Preferential syntheses of semiconducting vertically aligned single-walled carbon nanotubes for direct use in FETs," *Nano Lett.*, **9**, 2682 (2008).

[12] A. R. Harutyunyan, G. Chen, T. M. Paronyan, E. M. Pigos, O. A. Kuznetsov, K. Hewaparakrama, S. M. Kim, D. Zakharov, E. A. Stach, and G. U. Sumanasekera, "Preferential growth of single-walled carbon nanotubes with metallic conductivity," *Science*, **326**, 116 (2009).

[13] W. –H. Chiang and R. M. Sankaran, "Linking catalyst composition to chirality distribution

of as-grown single-walled carbon nanotubes by tuning NixFe1-x nanoparticles," *Nature Mater*., **8**, 882 (2009).

[14] A. Hashimoto, K. Suenaga, A. Gloter, K Urita, and S. Iijima, "Direct evidence for atomic defects in grapheme layers," *Nature*, **430**, 870 (2004).

[15] J. M. Zuo, I. Vartanyants, M. Gao, R. Zhang, L. A. Nagahara, "Atomic resolution imaging of a carbon nanotube from diffraction intensities," *Science*, **300**, 1419 (2003).

[16] S. Reich, L. Li, and J. Robertson, "Control the chirality of carbon nanotubes by epitaxial growth," *Chem. Phys. Lett*., **421**, 469 (2006).

[17] E. R. Meshot, and A. J. Hart, "Abrupt self-termination of vertically aligned carbon nanotube growth," *Appl. Phys. Lett*., **92**, 113107 (2008).

[18] D. N. Futaba, K. Hata, T. Yamada, K. Mizuno, M. Yumura, and S. Iijima, "Kinetics of water-assisted single-walled carbon nanotube synthesis revealed by a time-evolution analysis," *Phys. Rev. Lett*., **95**, 056104 (2005).

[19] T. Yamada, A. Maigne, M. Yudasaka, K. Mizuno, D. N. Futaba, M. Yumura, S. Iijima, and K. Hata, "Revealing the secret of water-assisted carbon nanotube synthesis by microscopic observation of the interaction of water on the catalysts," *Nano Lett.*, **8**, 4288 (2008).

[20] P. B. Amama, C. L. Pint, L. McJilton, S. M. Kim, E. A. Stach, P. T. Murray, R. H. Hauge, and B. Maruyama, "Role of water in super growth of single-walled carbon nanotube carpets," *Nano Lett*., **9**, 44 (2009).

[21] S. M. Kim, C. L. Pint, P. B. Amama, R. H. Hauge, B. Maruyama, and E. A. Stach, "Catalyst and catalyst support morphology evolution in single-walled carbon nanotube supergrowth: Growth deceleration and termination," *J. Mater. Res*., **25**, 1875 (2010).

[22] S. M. Kim, C. L. Pint, P. B. Amama, D. N. Zakharov, R. H. Hauge, B. Maruyama, and E. A. Stach, "Evolution in catalyst morphology leads to carbon nanotube growth termination," *J. Phys. Chem. Lett*., **1**, 918 (2010).

[23] W. Cho, M. Schulz, and V. Shanov, "Growth termination mechanism of vertically aligned centimeter long carbon nanotube arrays," *Carbon*, **69**, 609 (2014).

[24] M. Stadermann, S. P. Sherlock, J. –B. In, F. Fornasiero, H. G. Park, A. B. Artyukhin, Y. Wang, J. J. D. Yoreo, C. P. Grigoropoulos, O. Bakajin, A. A. Chernov, and A. Noy, "Mechanism and kinetics of growth termination in controlled chemical vapor deposition growth of multiwall carbon nanotube arrays," *Nano Lett*., **9**, 738 (2009).

[25] P. B. Amama, C. L. Pint, S. M. Kim, L. McJilton, K. G. Eyink, E. A. Stach, R. H. Hauge,

and B. Maruyama, “Influence of alumina type on the evolution and activity of alumina-supported Fe catalysts in single-walled carbon nanotube carpet growth,” *ACS Nano*, **4**, 895 (2010).

[26] K. Hata, D. N. Futaba, K. Mizuno, T. Namai, M. Yumura, and S. Iijima, “Water-assisted highly efficient synthesis of impurity-free single-walled carbon nanotubes,” *Science*, **306**, 1362 (2004).

[27] W. Cho, M. Schulz, and V. Shanov, “Growth and characterization of vertically aligned centimeter long CNT arrays,” *Carbon*, **72**, 264 (2014).

[28] J. Lee, E. Oh, T. Kim, J. –H. Sa, S. –H. Lee, J. Park, D. Moon, I. S. Kang, M. J. Kim, S. M. Kim, and Lee, K.-H. “The influence of boundary layer on the growth kinetics of carbon nanotube forests,” *Carbon*, **93**, 217 (2015).

[29] M. Kumar, and Y. Ando, “Chemical vapor deposition of carbon nanotubes: a review on growth mechanism and mass production,” *J. Nanosci. Nanotechnol.*, **10**, 3739 (2010).

List of Publications and Significant Collaborations that resulted from your AOARD supported project:

- S. J. Jeong, J. Lee, H. Kim, J. Y. Hwang, B Ku, D. N. Zakharov, B. Maruyama, E. A. Stach, and S. M. Kim, “Direct Observation on Morphological Evolution of Catalyst during Carbon Nanotube Forest Growth: New Insights for Growth and Growth Termination,” submitted to ACS Nano.
- Frequent research discussions over phone or emails with Dr. Benji Maruyama at AFRL